Title

Lineage Tracing and Cell Ablation Identify a Post-Aire-Expressing Thymic Epithelial Cell Population

Journal

Cell Reports, 5(1)

ISSN

2639-1856

Authors

Metzger, Todd C
Khan, Imran S
Gardner, James M
et al.

Publication Date

2013-10-01

DOI

10.1016/j.celrep.2013.08.038

Peer reviewed

Published in final edited form as:
Cell Rep. 2013 October 17; 5(1): . doi:10.1016/j.celrep.2013.08.038.

Lineage tracing and cell ablation identifies a post-Aire expressing thymic epithelial cell population

Todd C. Metzger[1], **Imran S. Khan**[1], **James M. Gardner**[1,2], **Maria L. Mouchess**[1], **Kellsey P. Johannes**[1], **Anna K. Krawisz**[1], **Katarzyna M. Skrzypczynska**[1], and **Mark S. Anderson**[1]

[1]Diabetes Center, University of California, San Francisco, San Francisco, CA 94143-0540, USA

[2]Department of Surgery, University of California, San Francisco, San Francisco, CA 94143-0540, USA

Abstract

Thymic epithelial cells in the medulla (mTECs) play a critical role in enforcing central tolerance through expression and presentation of tissue-specific antigens (TSAs) and deletion of autoreactive thymocytes. TSA expression requires autoimmune regulator (Aire), a transcriptional activator present in a subset of mTECs characterized by high CD80 and MHC II expression and a lack of potential for differentiation or proliferation. Here, using an *Aire-DTR* transgenic line, we show that short-term ablation specifically targets Aire^{+} mTECs, which quickly undergo RANK-dependent recovery. Repeated ablation also affects Aire^{-} mTECs, and using an inducible *Aire-Cre* fate-mapping system, we find that this results from the loss of a subset of mTECs that showed prior expression of Aire, maintains intermediate TSA expression, and preferentially migrates towards the center of the medulla. These results clearly identify a distinct stage of mTEC development and underscore the diversity of mTECs that play a key role in maintaining tolerance.

Central tolerance in the thymus plays a critical role in preventing T cell reactivity to self and the prevention of autoimmunity (Stritesky et al., 2012). Medullary thymic epithelial cells (mTECs) are a specialized antigen presenting cell type for guiding central tolerance, which they enforce through their expression of a wide array of tissue-specific self-antigens (TSAs) (Derbinski et al., 2001, Metzger and Anderson, 2011). TSA expression depends in part on *Aire* (Anderson et al., 2002), which was originally identified as the defective gene in the monogenic, multi-organ autoimmune syndrome Autoimmune Polyglandular Syndrome Type 1 (APS1) (Consortium, 1997, Nagamine et al., 1997). While the molecular mechanisms by which Aire enables TSA expression in mTECs are not fully elucidated, many individual Aire-dependent TSAs have unique roles for enforcing central tolerance (DeVoss et al., 2006, Shum et al., 2009, Su et al., 2012). Early reports found that transgenic Aire-dependent antigen expression enforced central tolerance primarily through negative selection (Liston et al., 2003, Anderson et al., 2005), and later reports found that endogenous Aire-dependent antigens can also mediate efficient negative selection of autoreactive epitope-specific T cell clones in a polyclonal setting (DeVoss et al., 2006, Taniguchi et al., 2012). More recently, transgenic and endogenous Aire-dependent antigens have also been found to serve as

Correspondence: manderson@diabetes.ucsf.edu; ph. (415) 502-8052, fax (415) 564-5813.

ligands for regulatory T cell (Treg) induction (Aschenbrenner et al., 2007, Malchow et al., 2013).

Expression of Aire in the postnatal state has been found predominantly within a subset of mTECs (Heino et al., 1999, Zuklys et al., 2000, Derbinski et al., 2001, Gray et al., 2007), consistent with its critical role in central tolerance induction. The Aire^{+} mTEC subset uniformly exhibits high MHC Class II and CD80 expression (Gabler et al., 2007, Gray et al., 2007) and is thought to be most important for enforcing negative selection of autoreactive thymocytes, while Aire^{-} mTEC subsets can express both high and low amounts of these markers. Given the observations that MHC II^{lo} mTECs precede MHC II^{hi} mTECs during ontogeny (Gabler et al., 2007, Hamazaki et al., 2007) and can give rise to MHC II^{hi} mTECs in *in vitro* cultures (Rossi et al., 2007, Gray et al., 2007), MHC II^{lo} mTECs appear to represent a precursor of Aire^{+} mTECs. In line with this precursor-product relationship, many Aire^{-} mTECs are actively dividing in a steady-state adult thymus, and presumably replace non-dividing Aire^{+} mTECs, which undergo a substantial amount of turnover and replacement (Gray et al., 2007, Gabler et al., 2007). However, other evidence has suggested that Aire may mark an mTEC subset with further differentiation potential (Gillard et al., 2007, Yano et al., 2008, Nishikawa et al., 2010, Wang et al., 2012).

A number of signaling components converging on NF-κB activation appear to play an important role in mTEC development, particularly the TNF receptor family members RANK and CD40, which signal through TRAF6 (Akiyama et al., 2005, Rossi et al., 2007, Akiyama et al., 2008, Hikosaka et al., 2008, White et al., 2008). Crosstalk between developing stromal cells and lymphoid cells bearing ligands for these receptors is required for proper mTEC differentiation (Rossi et al., 2007). Additional signals, including ligands operating through the lymphotoxin β receptor, also contribute to proper mTEC development and homeostasis (Boehm et al., 2003, White et al., 2010). Despite the clear requirement for these pathways in development, their role in the regulation of the adult mTEC compartment, which undergoes both homeostatic turnover and phases of involution and recovery following infection (Ross et al., 2012), remains undefined.

Here, we utilized genetic ablation and fate-mapping techniques to examine the role of Aire in the development and maintenance of the mTEC compartment at baseline and in response to dynamic changes. We developed an *Aire*-regulated bacterial artificial chromosome (BAC) transgenic mouse line that drives the expression of the high affinity diphtheria toxin receptor (DTR) to allow controlled ablation of Aire-expressing cells *in vivo*. Treatment of *Aire-DTR* transgenic mice with diphtheria toxin (DT) demonstrated that Aire-expressing mTECs are efficiently ablated, but long term DT treatment of *Aire-DTR* mice resulted in ablation of the entire mTEC compartment and loss of immune tolerance. Detailed fate mapping experiments with a novel inducible *Aire-Cre* mouse strain revealed a large and unique population of post-Aire expressing mTECs. These post-Aire mTECs maintained intermediate Aire-dependent TSA expression but reduced their expression of mTEC maturation markers and became more centrally located within the medulla. Finally, DT-mediated mTEC ablation revealed a remarkable regenerative potential of mTECs to repopulate the thymus in a RANK-dependent manner.

Results

An *Aire-DTR* mouse allows targeted ablation of Aire^{+} mTECs

The importance of Aire in mediating selection events led us to create a transgenic mouse expressing the human DTR (also known as heparin-binding EGF-like growth factor) under the transcriptional control of Aire (*Aire-DTR*), in order to allow temporal control of Aire^{+} mTEC apoptosis following diphtheria toxin (DT) administration (Jung et al., 2002, Kim et

al., 2007). A previously characterized DTR-GFP construct (Jung et al., 2002, Kim et al., 2007) was placed under control of the Aire promoter using a BAC (Gardner et al., 2008) (Figure 1A). In *Aire-DTR* mice, DTR-GFP was expressed specifically by mTECs within the thymus, and co-localized with Aire by immunofluorescence (Figure 1B). An initial assessment of DT-mediated ablation showed complete loss of Aire-expressing cells following a single injection of DT (Figure 1B), and a titration of DT dosing revealed a dose-response curve that was similar to that observed in other DTR ablation systems (Jung et al., 2002, Kim et al., 2007) (Figure 1C). Flow cytometric analysis confirmed that GFP expression was specific to the MHC II^{hi} mTEC subset, and that GFP+ mTECs were efficiently ablated with a single dose of DT (Figure 1D). We also observed some loss of GFP- mTECs with DT treatment, although the weakness of signal from the DTR fusion protein, as seen in other DTR systems (Jung et al., 2002, Meredith et al., 2012), underreported Aire expression to some extent (T.C.M. and I.S.K., unpublished data). Importantly, the MHC II^{lo} fraction of mTECs remained intact after a single DT treatment. Outside of the thymus, we also observed DT-mediated ablation of extrathymic Aire-expressing cells (eTACs), a rare population present in secondary lymphoid organs (Gardner et al., 2008) (T.C.M. and J.M.G., unpublished data). For clarity, we chose to focus our initial experimental efforts on the mTEC compartment.

Extended $Aire^+$ mTEC ablation depletes all mTEC subsets

We next sought to determine the effects of continuous $Aire^+$ mTEC ablation on the architecture and cellularity of the mTEC compartment. We administered DT every 48 hours to a cohort of *Aire-DTR* mice, analyzed GFP+ mTEC ablation at various time-points after the beginning of treatment, and found that GFP+ mTECs were still completely ablated after five rounds of DT treatment. However, we observed recovery of GFP+ mTECs with DT treatment beyond this time-point (T.C.M., unpublished data), presumably due to antibody-mediated DT neutralization (Buch et al., 2005). Thus, we chose to use a 9-day ablation time-course, and found that repeated $Aire^+$ mTEC ablation led to a substantial loss of cytokeratin 5+ mTECs (Figure 2A), with depletion of both GFP^- MHC II^{hi} mTECs as well as MHC II^{lo} mTECs (Figure 2B, 2C). Interestingly, despite the absence of mTECs from these mice, $CD4^+$ thymocytes and $CD11c^+$ DCs were still observed throughout the medulla (Figure 2D). Total cell counts between ablated and control mice were similar, indicating that ablation in the *Aire-DTR* mouse was specific to mTECs and did not lead to a dramatic loss of thymocytes (Figure 2E).

mTEC ablation leads to impaired $CD4^+$ T cell selection

To examine the effects of mTEC ablation on ongoing thymic selection in a polyclonal setting, we again continuously ablated mTECs over 9 days, and observed a substantial increase in the proportion of CD4 single-positive (SP) thymocytes within mTEC-ablated thymi (Figure 3A), consistent with defective negative selection of a subset of the developing T cell pool in the absence of the mTEC compartment. Furthermore, we observed that the proportion of developing $Foxp3^+$ Tregs among CD4 SP cells in the thymus was decreased (Figure 3B), although this was partially counterbalanced by the overrepresentation of total CD4 SP events in mTEC-ablated mice.

We next turned to the *RIP-mOVA* model of neo-self-antigen expression within $Aire^+$ mTECs, in which the rat insulin promoter drives expression of the model antigen ovalbumin (OVA) in a membrane-bound form and examined how mTEC ablation affected negative selection of the OVA-specific *OT-II* $CD4^+$ TCR transgenic line (Anderson et al., 2005). We analyzed thymocytes from *OT-II*, *OT-II RIP-mOVA* and *OT-II RIP-mOVA Aire-DTR* mice that had received repeated DT treatments, and found that *OT-II RIP-mOVA* mice had dramatically reduced CD4 SP events, as reported previously (Anderson et al., 2005). In

contrast, mTEC ablation in *OT-II RIP-mOVA Aire-DTR* mice completely removed *OT-II* mediated negative selection, and CD4 SP T cell development in *OT-II* and *OT-II RIP-mOVA Aire-DTR* mice was indistinguishable (Figure 3C). Furthermore, the development of Tregs observed in the presence of thymic OVA was also lost with mTEC ablation and the removal of cognate antigen from the thymus (Figure 3D). Finally, antibodies specific for the TCR chains of the *OT-II* TCR confirmed that, while negative selection in *RIP-mOVA* mice led to a lower frequency and intensity of the *OT-II* TCR, *OT-II* T cells with normal antigen affinity developed in the absence of mTECs (Figure S1). Taken together, these results demonstrate that transgenic ablation of mTECs in the adult thymus leads to a loss of proper selection in both polyclonal and transgenic settings.

We next returned to a polyclonal setting to look for functional defects in tolerance resulting from mTEC ablation. Initially, we treated mice from birth, as central tolerance induction to Aire-dependent antigens is most critical at this stage (Guerau-de-Arellano et al., 2009). While others have reported a lack of non-specific DT toxicity in newborn mice (Kim et al., 2007), treatment of mice starting from birth was lethal in our mouse colony (T.C.M., unpublished data). We next treated mice beginning at one week of age, and found that weight gain by the treated mice slowed towards the end of the treatment regimen (Figure 3E), but that the mice survived and gained weight normally after weaning. We monitored the mice up to 14 weeks of age, and observed a substantial increase in the proportion of $CD44^+$ $CD62L^-$ memory/effector T cells in the periphery at this timepoint (Figure 3F), suggesting increased leakage of autoreactive T cells from the thymus following mTEC ablation. Unlike the decreased proportions of thymic Tregs we observed immediately following mTEC ablation, we found increased percentages of peripheral Tregs in mice that had experienced mTEC ablation before weaning (Figure 3G). Lastly, we observed a significant increase in tissue infiltrates of lacrimal glands (Figure 3H), demonstrating that mTEC ablation in the postnatal thymus leads to a functional break in tolerance.

Lineage tracing identifies a post-Aire, MHC II^{lo} stage of mTEC development

Our observation that repeated DT-mediated ablation of $Aire^+$ mTECs led to ablation of mTECs outside of this pool led us to address whether or not there might be a post-Aire stage of mTEC development. Towards this end, we created an inducible *Aire-Cre* line in which tamoxifen treatment would allow nuclear localization and loxP-directed excision in *Aire*-expressing cells (Figure 4A). Because transient *Aire* expression occurs during embryogenesis (Nishikawa et al., 2010), we used a previously described approach of dual flanking of the Cre recombinase with tamoxifen receptor cassettes to allow strict temporal control of Cre activity (Matsuda and Cepko, 2007). We then crossed these mice with a mouse strain harboring Cre-inducible TdTomato (RFP) under control of the ubiquitous Rosa26 promoter to generate mice where Aire-expressing cells would be irreversibly labeled through constitutive RFP expression following tamoxifen treatment. Lineage tracing mice were treate with tamoxifen, and we observed strong RFP labeling of a subset of EpCAM+ mTECs (Figure 4B). RFP-labeled cells had a high degree of co-staining with nuclear Aire protein as expected (Figure 4C) and, importantly, we saw no evidence of RFP labeling in the absence of tamoxifen treatment (Figure 4B, 4C), indicating the absence of background Cre activity.

We next addressed the developmental fate of $Aire^+$ mTECs by delivering a single dose of tamoxifen and analyzing the characteristics of RFP-labeled mTECs over time. We observed a high degree of co-expression of RFP and Aire-driven GFP at only 24 hours post-tamoxifen treatment (Gardner et al., 2008) (Figure 5A), demonstrating highly specific labeling of $Aire^+$ mTECs at day 0. However, when we examined Aire-GFP expression by RFP^+ mTECs a week or more after a single dose of tamoxifen treatment, we found that many labeled mTECs were no longer actively expressing Aire, and that roughly half of all labeled mTECs

progressed to this post-Aire stage within 10 days (Figure 5B). Importantly, we found that the overall decay in labeled Aire$^+$ GFP$^+$ cells showed a half-life of about 7 days, consistent with previous reports (Gray et al., 2007), but when post-Aire cells were taken into account, labeled cells remained present in relatively stable proportions within the first week of labeling (Figure 5B). Nevertheless, at one week after labeling, post-Aire mTECs decayed at the previously reported rate, suggesting a lack of further differentiation or expansion capacity among this population. We also examined MHC Class II expression on post-Aire mTECs and found that, in addition to losing expression of Aire-GFP signal and Aire protein (Figure S2A), a substantial fraction of post-Aire mTECs could also revert to an MHC II^{lo} phenotype (Figure 5C). By immunofluorescent staining, we again found that while Aire-GFP, RFP, and nuclear Aire protein co-localize shortly after tamoxifen treatment, by day 7 post-tamoxifen many post-Aire cells express only RFP (Figure 5D). Post-Aire cells at 21 days after labeling continued to be localized to the medulla, and while Aire and Aire-GFP signals tended to outline the edge of the medullary region, as shown previously (Zuklys et al., 2000, Yano et al., 2008), post-Aire RFP cells appeared to be preferentially localized towards the center of the medulla by 2D and 3D imaging (Figure S2B, S2C). We further investigated the differential localization of Aire$^+$ and post-Aire mTECs 21 days after labeling and found that while Aire$^+$ mTECs were preferentially localized to the outer portion of the medulla, as described previously (Irla et al., 2013, Yano et al., 2008), post-Aire mTEC distribution was skewed towards the center of the medulla (Figure 5E-H).

Given the phenotypic similarity between MHC II^{lo} post-Aire mTECs and the potential mTEC progenitor population, we sought to directly assess the potential of post-Aire mTECs to contribute to mTEC cellularity followed DT-mediated mTEC ablation. We labeled Aire$^+$ mTECs through tamoxifen treatment, waited for a fraction of labeled mTECs to turn off Aire expression, and then ablated remaining Aire$^+$ mTECs through the *Aire-DTR* transgene (Figure S2D). In line with the homeostatic decay of post-Aire mTECs, we observed that RFP-labeled mTECs were relatively scarce after recovery from a single DT ablation (Figure S2E), thus further supporting a linear relationship between Aire$^-$ mTEC precursors, Aire$^+$ mTECs, and a final, distinct post-Aire state.

Post-Aire mTECs lose maturation markers but maintain intermediate TSA expression

Aire expression in mTECs is critical for the proper expression of TSAs within the thymus (Anderson et al., 2002). Thus, we addressed whether TSA expression occurred only in mTECs that were actively co-expressing Aire, as suggested in an approach where relatively long-lived LacZ activity was used to identify post-Aire cells (Wang et al., 2012), or whether Aire might permit the further differentiation of mTECs into a post-Aire, TSA-expressing state (Farr et al., 2002, Yano et al., 2008). We identified post-Aire mTECs by sorting out MHC II^{lo} RFP+ mTECs, which uniformly lack Aire protein (Figure 6A), 7 days after a single tamoxifen labeling and compared gene expression with other mTEC fractions. Importantly, expression of Aire and MHC II at the transcript level mirrored our observations at the protein level, and the expression patterns of the maturation markers CD80 and CD86 were also consistent with the loss of a mature phenotype by post-Aire mTECs (Figure 6B). We also found that involucrin (Ivl), a marker suggested to identify the last stages of mTEC development (Yano et al., 2008, White et al., 2010, Wang et al., 2012), was markedly increased in the post-Aire lineage. Lastly, we addressed relative TSA expression by post-Aire, MHC II^{lo} mTECs and other mTEC subsets, and found that post-Aire mTECs continued maintain substantially higher TSAs expression than RFP-MHC II^{lo} mTECs, which were enriched for pre-Aire mTECs (Figure 6C). Importantly, post-Aire mTECs had lower TSAs expression than the mature, Aire$^+$ mTEC-containing subset, which suggests a direct role for Aire in facilitating TSA expression but not maintaining it. These results identify post-Aire MHC II^{lo} mTECs as a population with distinct TSA and antigen-

presenting capabilities, which may indicate a unique role for this population in driving central tolerance.

RANK signaling controls Aire$^+$ mTEC homeostasis and regeneration

While previous reports have noted a capacity for involution and regeneration by thymic epithelial cells in response to pharmaceutical agents (Fletcher et al., 2009), direct ablation and recovery of mTECs has not yet been addressed. We thus returned to a short-term DT-mediated ablation of Aire$^+$ mTECs to address the regulation of Aire$^+$ mTEC development in the adult thymus. Following a single ablation of Aire$^+$ mTECs (Figure 7A), we observed that a substantial number of Aire$^+$ GFP$^+$ mTECs were regenerated within three days (Figure 7B). Furthermore, FACS analysis of thymi at several stages of recovery revealed that mTEC subset ratios had returned to normal proportions within a week of ablation (Figure 7C). Prior studies have suggested that Aire$^+$ mTECs develop from an immature MHC II^{lo} CD80$^-$ precursor population via an MHCII^{hi} Aire$^-$ intermediate stage, (Gray et al., 2007, Rossi et al., 2007), and in line with these observations, we addressed whether or not mTEC recovery might be impaired after a longer DT-mediated ablation regimen in which all subsets of mTEC are ablated. In line with these studies, we found that the additional loss of Aire$^-$ mTECs with repeated DT treatment led to an impaired recovery potential seven days after cessation of the repeated DT regimen (Figure 7D-F). Importantly, we observed that ablated mTECs were ultimately able to recover to the same extent as their wild-type controls, suggesting that repeated DT treatment quantitatively but not qualitatively affects the recovery potential of mTECs.

RANK signaling through TRAF6 is an important mediator of Aire$^+$ mTEC development (Akiyama et al., 2005, Rossi et al., 2007, Akiyama et al., 2008, Hikosaka et al., 2008), but the importance of this pathway has been established primarily during thymic organogenesis. In order to determine the contribution of RANK signaling to the recovery of Aire$^+$ mTECs in adult mice, we blocked RANK signaling with an anti-RANK ligand antibody during recovery from a single DT treatment (Figure 7G). Interestingly, we found that blockade of this pathway substantially reduced the proportion of Aire$^+$ mTECs present in control mice after five days of RANK signaling blockade (Figure 7G), consistent with a high degree of constitutive Aire$^+$ mTEC turnover (Gray et al., 2007) and a requirement for RANK signaling in this process. In the context of recovery from Aire$^+$ mTEC ablation, we observed that isotype-treated mice recovered completely, and exhibited the previously reported phenomenon of Aire$^+$ mTEC overshoot (Fletcher et al., 2009), which was more apparent than when indirectly assessing Aire expression through GFP (Figure 7C). Additionally, the effect of RANK signaling blockade was more dramatic in the context of recovery from DT-mediated Aire$^+$ mTEC ablation, as this process was completely blocked in the absence of RANK signaling (Figure 7G). Finally, we assessed the proliferative response of mTEC subsets during mTEC recovery by Ki67 staining, and found that RANK signaling was required to allow enhanced proliferation of Aire$^-$ mTEC subsets during ablation recovery (Figure 7H). Taken together, these results identify a striking capacity for RANK-dependent Aire$^+$ mTEC induction and repopulation of the adult thymus.

Discussion

Since the original identification of mTECs as the source of both Aire and TSAs (Heino et al., 1999, Derbinski et al., 2001), there has been debate about the role of Aire and of epithelial cell maturation in driving TSA expression (Anderson et al., 2002, Farr et al., 2002), and the relationship of Aire$^+$ and Aire$^-$ mTECs has remained unclear. Here, using two separate genetic systems, we have shown that: (1) repeated ablation of Aire$^+$ mTECs leads to an unexpected loss of Aire$^-$ mTEC subsets; (2) following Aire induction, Aire is downregulated in a final post-Aire mTEC stage that retains intermediate TSA expression

and acquires a distinct anatomical localization with the medulla; and (3) the recovery potential of Aire$^+$ mTECs during adulthood depends on RANK signaling and correlates with the availability of precursor MHC II^{lo} cells.

Aire$^-$ mTECs are lost following repeated Aire$^+$ mTEC ablation

To investigate the relationships of Aire$^+$ and Aire$^-$ mTEC subsets, we created an *Aire-DTR* mouse in which Aire$^+$ mTEC ablation could be temporally controlled. We found that while a single DT treatment caused specific ablation of mature mTECs, repeated DT-mediated ablation led to a loss of the putative immature mTEC population as well. This was not a result of general thymic atrophy, as total thymic cellularity remained unchanged, and both thymocytes and DCs continued to fill the medulla. In contrast to evidence that Aire$^+$ mTECs represent a terminally differentiated population (Gray et al., 2007), these results suggested that Aire+ mTECs could contribute to the MHC II^{lo} pool of mTECs. In fact, recent experiments with a constitutive *Aire-Cre* have indicated that Aire$^+$ mTECs may adopt a more immature phenotype (Nishikawa et al., 2010), although the specificity of labeling in this approach was unclear.

Antigens expressed by mTECs may be handed off to and presented by DCs (Koble and Kyewski, 2009), and such indirect presentation can compensate for the lack of direct presentation by mTECs (Aichinger et al., 2013). Therefore, it was unclear whether mTEC ablation over the timespan of 9 days would be sufficient to remove functionally relevant mTEC-derived antigens from the thymus, or whether such antigens might persist and continue to be presented by DCs. To test the functional effects of mTEC ablation, we first examined polyclonal thymocytes, and found that CD4 SP thymocytes were over-represented in conditions of mTEC ablation, similar to prior observations in mice with mTEC-directed reductions in MHC II expression (Hinterberger et al., 2010). These results suggested that a substantial proportion of thymocytes, which would otherwise undergo deletion, were instead surviving in the absence of mTEC-derived antigen. The loss of negative selection to mTEC-derived antigen became much more striking when we performed similar experiments in the context of RIP-mOVA-mediated deletion of OT-II T cells, a model in which antigen handoff may contribute to negative selection (Hubert et al., 2011, Gallegos and Bevan, 2004). Importantly, this result determined that antigen handoff and/or persistence among DCs was not sufficient to mediate detectable negative selection during the duration of mTEC ablation that we induced.

Finally, we found that mTEC ablation in a polyclonal setting prior to weaning led to autoimmunity in adulthood. It should be noted that eTAC ablation could have contributed to the observed autoimmunity, although lack of specific TSA expression in the thymus likely explains our observation of lacrimal gland autoimmunity (DeVoss et al., 2010). Interestingly, lacrimal autoimmunity has been one of the more penetrant phenotypes with a lack of proper Aire function (Su et al., 2008), and we expect that more extensive autoimmunity would have been observed if earlier DT administration was feasible (Guerau-de-Arellano et al., 2009). Taken together, these results show that mTEC ablation in the *Aire-DTR* mouse leads to a loss of negative selection to mTEC-expressed antigens, and further highlights the critical role of mTECs in providing unique ligands for thymic negative selection.

Aire$^+$ mTECs lose Aire and MHC II in a final post-Aire stage

By developing an inducible *Aire-Cre* mouse, we were able to specifically label Aire-expressing cells with constitutive RFP expression and follow the developmental fate of these cells. In contrast to previous reports with a germline *Aire-Cre* labeling system (Nishikawa et al., 2010), our labeling was highly specific to cells actively expressing Aire within 24 hours

of tamoxifen-induced labeling. However, by immunofluorescence and flow cytometry, we observed that a substantial portion of Aire$^+$ mTECs lost Aire expression within a week of labeling, and many of these post-Aire mTECs adopted an MHC II^{lo} "immature" phenotype. Furthermore, we found a change in the distribution of post-Aire cells within the medulla after 21 days of labeling. Over 10% of all mTECs adopted a post-Aire fate in our experiment, which underestimates the total proportion of post-Aire mTECs due to incomplete and temporally restricted labeling of Aire$^+$ mTECs. The identification of a post-Aire mTEC developmental stage explains at least in part our observation that continued ablation of Aire$^+$ mTECs leads to a loss outside of the Aire+ mTEC compartment. We followed post-Aire mTECs during homeostatic and ablation recovery conditions, and in both, observed that post-Aire cells did not contain regenerative potential. Thus, our observation of a post-Aire mTEC state was consistent with our observations in the DT-mediated mTEC ablation and recovery, in that non-Aire$^+$ mTECs could be ablated, or prevented from forming, through continued DT treatment, but the fundamental regenerative capacity of mTECs was not dependent on the Aire$^+$ subset.

Loss of Aire by mTECs is consistent with a model in which Aire drives further maturation of the mTEC subset (Gillard et al., 2007). However, we found that Aire-dependent TSA expression was highest in MHC II^{hi} cells, and decreased following transition of post-Aire mTECs into the MHC II^{lo} state. Thus, at least in terms of TSA expression, Aire seems to directly drive or stabilize expression of these transcripts (Abramson et al., 2010), rather than facilitate transition into a specialized TSA-expressing post-Aire cell. In line with this, recent work has found that TSAs expressed endogenously in the pancreas do not require canonical pancreatic differentiation factors for thymic expression (Danso-Abeam et al., 2013). Nevertheless, the persistence of TSA expression beyond the expression of Aire itself suggests that post-Aire mTECs may have a role in inducing tolerance to TSAs, and could explain detection of TSAs among Aire$^-$ mTECs (Derbinski et al., 2005, Derbinski et al., 2008, Villasenor et al., 2008). While TSA persistence in post-Aire mTECs could reflect different half-lifes of Aire and TSA transcripts, TSA persistence may also be related to suggested mechanisms of Aire function in which Aire acts to open TSA loci through epigenetic modification rather than directly binding and driving transcription at target loci (Abramson et al., 2010). Interestingly, we found that while canonical mTEC maturation markers including CD80 and MHC class II were decreased in post-Aire mTECs, involucrin, a potential marker of a post-Aire state (Yano et al., 2008, White et al., 2010), was in fact enriched in our post-Aire cells. Thus, the post-Aire mTEC developmental stage has a distinct transcriptional profile from the general pool of MHC II^{lo} mTECs, despite being indistinguishable by general maturation markers.

The lower amounts of TSAs and antigen presentation capabilities in post-Aire mTECs suggests this developmental state may support a feature of central tolerance other than negative selection of autoreactive T cells. Instead, such post-Aire cells may provide architectural cues to the maintenance of the thymic medulla, and we have observed altered localization of post-Aire mTECs within the medulla. Indeed, the loss of the entire medullary compartment with extended ablation of Aire$^+$ mTECs may have occurred not only due to the loss of both Aire+ and post-Aire mTECs, but also from a loss of important organizational cues provided by post-Aire mTECs. Proper architectural organization is likely required for appropriate regulatory T cell induction, as recent work has shown that altered orientation of medullary components in the absence of XCL1 chemokine signals leads to impaired regulatory T cell induction (Lei et al., 2011). Furthermore, we speculate that post-Aire mTECs may also have a direct role in induction of regulatory T cells, consistent with the lack of regulatory T cells following extensive ablation of both Aire$^+$ and post-Aire mTEC in *OT-II* transgenic and polyclonal models. The reduced expression of both MHC II and antigen on post-Aire mTECs may promote regulatory T cell survival over deletion or

neglect, and in line with a requirement for intermediate TCR signaling in regulatory T cell development, recent work has shown that the partial inhibition of MHC Class II expression by mTECs leads to enhanced selection of regulatory T cells (Hinterberger et al., 2010).

RANK signaling controls Aire$^+$ mTEC homeostasis and regeneration

Our investigation into the recovery potential of mTECs in the adult mouse revealed a remarkable capacity of Aire+ mTECs to be regenerated following diphtheria toxin-mediated ablation of this mTEC subset. The ability of the Aire$^+$ mTEC pool to recover from targeted ablation was much more dramatic that both our own and prior estimates of the homeostatic turnover of this compartment (Gabler et al., 2007, Gray et al., 2007). We found that the regenerative capacity of the Aire$^+$ mTEC subset correlated with the presence of the MHC II^{lo} subset, as MHC II^{hi} mTECs remained underrepresented for at least one week following more thorough mTEC ablation. These results support a precursor-product relationship among at least a subset of mTECs within the MHC II^{lo} pool and Aire$^+$ mTECs.

We also found that recovery of the Aire+ mTEC subset following targeted ablation was critically dependent on signaling from RANK-L, as a blocking antibody to this ligand completely prevented the re-emergence of Aire$^+$ mTECs after DT treatment. Previously, it has been suggested that RANK signaling might be important predominantly during initial stages of mTEC development (White et al., 2008). However, the data here clearly demonstrate a significant contribution of RANK signaling to the homeostatic turnover of the Aire$^+$ mTEC subset in control, non-ablated adult mice, thus highlighting the importance of RANK signaling in the induction of Aire$^+$ mTECs in adulthood. Interestingly, our analysis of mTEC proliferation during recovery from diphtheria toxin ablation suggested that RANK signaling might allow the maturation and induction of Aire expression by controlling proliferation of precursor populations, as mTEC proliferation across all subsets was suppressed to homeostatic amounts in the absence of RANK signaling.

Taken together, these results demonstrate that the mTEC compartment is highly dynamic and provide evidence of rapid turnover and tight regulation of Aire expression. This coordinated expression and turnover may be critical for the maintenance of central tolerance. In this regard, the continued turnover and replacement of Aire mTECs may help ensure a broad display of TSAs to the developing T cell repertoire. Detailed analysis of TSA expression has demonstrated that this process is stochastic with a somewhat random distribution of TSAs in mTECs (Derbinski et al., 2008, Villasenor et al., 2008). Through rapid turnover and replacement of mTECs, random TSA expression in any single mTEC can still be anatomically and spatially spread out in the medullary compartment for the maintenance of tolerance to TSAs. Finally, our results make important modifications to the prevailing model of Aire$^+$ mTECs representing a terminally-differentiated cell population by identifying a post-Aire stage in which both Aire and maturation markers are lost. The existence of this post-Aire state suggests that future work addressing properties of mTEC subsets should seek to further identify pre- and post-Aire mTECs, and may help in more precisely identifying which mTEC subsets harbor the dramatic regenerative potential which we observed in our DT ablation system.

Experimental Procedures

Mice

Generation of Aire-DTR and Aire-Cre mice and sources of pre-existing strains is described in the Extended Experimental Procedures. All mice were housed in a specific-pathogen free facility at UCSF, and the UCSF Institutional Animal Care and Use Committee approved all experiments.

In vivo mouse treatments

Diphtheria toxin (DT, Sigma-Aldrich) was administered at a dose of 25–50 ng/g via i.p. injections for all experiments, with the exception of the RANK-L blocking experiment, in which DT was given via retro-orbital injections to mice anesthetized with a ketamine/xylazine mixture. RANK-L (clone IK22/5) or a Rat IgG2a isotype control (clone 2A3) were purchased from Bio-X-Cell and injected i.p. at 250 ug per dose as indicated. Tamoxifen (Sigma-Aldrich) was dissolved in corn oil (Sigma-Aldrich), and 2 mg doses were administered by oral gavage unless otherwise indicated. All treatments were performed on mice near 6–8 weeks of age.

Flow Cytometry

Thymocytes and splenocytes were isolated by, followed by red blood cell lysis for spleen samples. TECs were isolated by mincing and collagenase/dispase digestion (Gardner et al., 2008), followed by stromal cell enrichment on Percoll or Percoll PLUS gradients (GE Healthcare). Cells were blocked with 2.4G2 antibody at 20 ug/mL, and stained with the indicated surface marker antibodies (BioLegend). For intracellular staining, Anti-Aire-A647 (eBioscience) and anti-Ki67-PE (BD Biosciences) were used with the eBioscience Foxp3 / transcription factor buffer set. Cells were analyzed on BD LSRII and Fortessa cytometers, and cells were sorted on BD FACSAria III cytometers. Data was analyzed with BD FACS Diva and Flow Jo (Tree Star). FSC vs. SSC and DAPI dead cell exclusion was applied to non-fixed samples.

Quantitative PCR

Sorted cells were collected in a 50:50 mixture of DMEM and FBS, and RNA was extracted with a Qiagen RNeasy Micro kit, according to the manufacturer's instructions. cDNA was synthesized with an Invitrogen Superscript III kit, and inventoried Applied Biosystem Taqman gene expression assays were used for all targets. All targets were standardized to Cyclophilin A (*Ppia*) signals.

Statistical Analysis

Student's *t*-tests (two-tailed with Welch's correction) were performed using Microsoft Excel and Prism (Graph Pad). Analysis of mTEC densities was performed with a paired t-test.

Supplementary Material

Refer to Web version on PubMed Central for supplementary material.

Acknowledgments

We thank L. Jeker, T. LaFlam, and M. Cheng at UCSF for critical reading of the manuscript, D. Littman (NYU) for the eGFP-DTR construct, C. Cepko (Harvard) for the ERT2-Cre-ERT2 construct, H. Scott (U. Adelaide) for reagents, M. Krummel (UCSF) for mice, the UCSF Transgenic Core for help generating transgenic mice, the Diabetes Center Microscopy Core for assistance with Metamorph imaging, E. Oswald for assistance in sample preparation and the Biological Imaging Development Center at UCSF for technical assistance with 2-photon imaging. Supported by the US National Institutes of Health Grants AI097457 (M.S.A), K12-GM081266 (M.L.M.), DK063720 and DK59958 for core support, the Helmsley Charitable Trust (M.S.A, T.C.M), the American Diabetes Association (J.M.G.), and the UCSF Medical Scientist Training Program (I.S.K., J.M.G.).

References

Abramson J, Giraud M, Benoist C, Mathis D. Aire's partners in the molecular control of immunological tolerance. Cell. 2010; 140:123–135. [PubMed: 20085707]

Aichinger M, Wu C, Nedjic J, Klein L. Macroautophagy substrates are loaded onto MHC class II of medullary thymic epithelial cells for central tolerance. J Exp Med. 2013; 210:287–300. [PubMed: 23382543]

Akiyama T, Maeda S, Yamane S, Ogino K, Kasai M, Kajiura F, Matsumoto M, Inoue J. Dependence of self-tolerance on TRAF6- directed development of thymic stroma. Science. 2005; 308:248–251. [PubMed: 15705807]

Akiyama T, Shimo Y, Yanai H, Qin J, Ohshima D, Maruyama Y, Asaumi Y, Kitazawa J, Takayanagi H, Penninger JM, Matsumoto M, Nitta T, Takahama Y, Inoue J. The tumor necrosis factor family receptors RANK and CD40 cooperatively establish the thymic medullary microenvironment and self-tolerance. Immunity. 2008; 29:423–437. [PubMed: 18799149]

Anderson MS, Venanzi ES, Chen Z, Berzins SP, Benoist C, Mathis D. The cellular mechanism of Aire control of T cell tolerance. Immunity. 2005; 23:227–239. [PubMed: 16111640]

Anderson MS, Venanzi ES, Klein L, Chen Z, Berzins SP, Turley SJ, Von Boehmer H, Bronson R, Dierich A, Benoist C, Mathis D. Projection of an immunological self shadow within the thymus by the aire protein. Science. 2002; 298:1395–1401. [PubMed: 12376594]

Aschenbrenner K, D'cruz LM, Vollmann EH, Hinterberger M, Emmerich J, Swee LK, Rolink A, Klein L. Selection of Foxp3+ regulatory T cells specific for self antigen expressed and presented by Aire+ medullary thymic epithelial cells. Nat Immunol. 2007; 8:351–358. [PubMed: 17322887]

Boehm T, Scheu S, Pfeffer K, Bleul CC. Thymic medullary epithelial cell differentiation, thymocyte emigration, and the control of autoimmunity require lympho-epithelial cross talk via LTbetaR. J Exp Med. 2003; 198:757–769. [PubMed: 12953095]

Buch T, Heppner FL, Tertilt C, Heinen TJ, Kremer M, Wunderlich FT, Jung S, Waisman A. A Cre-inducible diphtheria toxin receptor mediates cell lineage ablation after toxin administration. Nat Methods. 2005; 2:419–426. [PubMed: 15908920]

Consortium F-GA. An autoimmune disease, APECED, caused by mutations in a novel gene featuring two PHD-type zinc-finger domains. Nat Genet. 1997; 17:399–403. [PubMed: 9398840]

Danso-Abeam D, Staats KA, Franckaert D, Van Den Bosch L, Liston A, Gray DH, Dooley J. Aire mediates thymic expression and tolerance of pancreatic antigens via an unconventional transcriptional mechanism. Eur J Immunol. 2013; 43:75–84. [PubMed: 23041971]

Derbinski J, Gabler J, Brors B, Tierling S, Jonnakuty S, Hergenhahn M, Peltonen L, Walter J, Kyewski B. Promiscuous gene expression in thymic epithelial cells is regulated at multiple levels. J Exp Med. 2005; 202:33–45. [PubMed: 15983066]

Derbinski J, Pinto S, Rosch S, Hexel K, Kyewski B. Promiscuous gene expression patterns in single medullary thymic epithelial cells argue for a stochastic mechanism. Proc Natl Acad Sci U S A. 2008; 105:657–662. [PubMed: 18180458]

Derbinski J, Schulte A, Kyewski B, Klein L. Promiscuous gene expression in medullary thymic epithelial cells mirrors the peripheral self. Nat Immunol. 2001; 2:1032–1039. [PubMed: 11600886]

Devoss J, Hou Y, Johannes K, Lu W, Liou GI, Rinn J, Chang H, Caspi RR, Fong L, Anderson MS. Spontaneous autoimmunity prevented by thymic expression of a single self-antigen. J Exp Med. 2006; 203:2727–2735. [PubMed: 17116738]

Devoss JJ, Leclair NP, Hou Y, Grewal NK, Johannes KP, Lu W, Yang T, Meagher C, Fong L, Strauss EC, Anderson MS. An autoimmune response to odorant binding protein 1a is associated with dry eye in the Aire-deficient mouse. J Immunol. 2010; 184:4236–4246. [PubMed: 20237294]

Farr AG, Dooley JL, Erickson M. Organization of thymic medullary epithelial heterogeneity: implications for mechanisms of epithelial differentiation. Immunol Rev. 2002; 189:20–27. [PubMed: 12445262]

Fletcher AL, Lowen TE, Sakkal S, Reiseger JJ, Hammett MV, Seach N, Scott HS, Boyd RL, Chidgey AP. Ablation and regeneration of tolerance-inducing medullary thymic epithelial cells after cyclosporine, cyclophosphamide, and dexamethasone treatment. J Immunol. 2009; 183:823–831. [PubMed: 19564346]

Gabler J, Arnold J, Kyewski B. Promiscuous gene expression and the developmental dynamics of medullary thymic epithelial cells. Eur J Immunol. 2007; 37:3363–3372. [PubMed: 18000951]

Gallegos AM, Bevan MJ. Central tolerance to tissue-specific antigens mediated by direct and indirect antigen presentation. J Exp Med. 2004; 200:1039–1049. [PubMed: 15492126]

Gardner JM, Devoss JJ, Friedman RS, Wong DJ, Tan YX, Zhou X, Johannes KP, Su MA, Chang HY, Krummel MF, Anderson MS. Deletional tolerance mediated by extrathymic Aire-expressing cells. Science. 2008; 321:843–847. [PubMed: 18687966]

Gillard GO, Dooley J, Erickson M, Peltonen L, Farr AG. Airedependent alterations in medullary thymic epithelium indicate a role for Aire in thymic epithelial differentiation. J Immunol. 2007; 178:3007–3015. [PubMed: 17312146]

Gray D, Abramson J, Benoist C, Mathis D. Proliferative arrest and rapid turnover of thymic epithelial cells expressing Aire. J Exp Med. 2007; 204:2521–2528. [PubMed: 17908938]

Guerau-De-Arellano M, Martinic M, Benoist C, Mathis D. Neonatal tolerance revisited: a perinatal window for Aire control of autoimmunity. J Exp Med. 2009; 206:1245–1252. [PubMed: 19487417]

Hamazaki Y, Fujita H, Kobayashi T, Choi Y, Scott HS, Matsumoto M, Minato N. Medullary thymic epithelial cells expressing Aire represent a unique lineage derived from cells expressing claudin. Nat Immunol. 2007; 8:304–311. [PubMed: 17277780]

Heino M, Peterson P, Kudoh J, Nagamine K, Lagerstedt A, Ovod V, Ranki A, Rantala I, Nieminen M, Tuukkanen J, Scott HS, Antonarakis SE, Shimizu N, Krohn K. Autoimmune regulator is expressed in the cells regulating immune tolerance in thymus medulla. Biochem Biophys Res Commun. 1999; 257:821–825. [PubMed: 10208866]

Hikosaka Y, Nitta T, Ohigashi I, Yano K, Ishimaru N, Hayashi Y, Matsumoto M, Matsuo K, Penninger JM, Takayanagi H, Yokota Y, Yamada H, Yoshikai Y, Inoue J, Akiyama T, Takahama Y. The cytokine RANKL produced by positively selected thymocytes fosters medullary thymic epithelial cells that express autoimmune regulator. Immunity. 2008; 29:438–450. [PubMed: 18799150]

Hinterberger M, Aichinger M, Prazeres Da Costa O, Voehringer D, Hoffmann R, Klein L. Autonomous role of medullary thymic epithelial cells in central CD4(+) T cell tolerance. Nat Immunol. 2010; 11:512–519. [PubMed: 20431619]

Hubert FX, Kinkel SA, Davey GM, Phipson B, Mueller SN, Liston A, Proietto AI, Cannon PZ, Forehan S, Smyth GK, Wu L, Goodnow CC, Carbone FR, Scott HS, Heath WR. Aire regulates the transfer of antigen from mTECs to dendritic cells for induction of thymic tolerance. Blood. 2011; 118:2462–2472. [PubMed: 21505196]

Irla M, Guenot J, Sealy G, Reith W, Imhof BA, Serge A. Threedimensional visualization of the mouse thymus organization in health and immunodeficiency. J Immunol. 2013; 190:586–596. [PubMed: 23248258]

Jung S, Unutmaz D, Wong P, Sano G, De Los Santos K, Sparwasser T, Wu S, Vuthoori S, Ko K, Zavala F, Pamer EG, Littman DR, Lang RA. In vivo depletion of CD11c+ dendritic cells abrogates priming of CD8+ T cells by exogenous cell-associated antigens. Immunity. 2002; 17:211–220. [PubMed: 12196292]

Kim JM, Rasmussen JP, Rudensky AY. Regulatory T cells prevent catastrophic autoimmunity throughout the lifespan of mice. Nat Immunol. 2007; 8:191–197. [PubMed: 17136045]

Koble C, Kyewski B. The thymic medulla: a unique microenvironment for intercellular self-antigen transfer. J Exp Med. 2009; 206:1505–1513. [PubMed: 19564355]

Lei Y, Ripen AM, Ishimaru N, Ohigashi I, Nagasawa T, Jeker LT, Bosl MR, Hollander GA, Hayashi Y, Malefyt Rde W, Nitta T, Takahama Y. Aire-dependent production of XCL1 mediates medullary accumulation of thymic dendritic cells and contributes to regulatory T cell development. J Exp Med. 2011; 208:383–394. [PubMed: 21300913]

Liston A, Lesage S, Wilson J, Peltonen L, Goodnow CC. Aire regulates negative selection of organ-specific T cells. Nat Immunol. 2003; 4:350–354. [PubMed: 12612579]

Malchow S, Leventhal DS, Nishi S, Fischer BI, Shen L, Paner GP, Amit AS, Kang C, Geddes JE, Allison JP, Socci ND, Savage PA. Aire-dependent thymic development of tumor-associated regulatory T cells. Science. 2013; 339:1219–1224. [PubMed: 23471412]

Matsuda T, Cepko CL. Controlled expression of transgenes introduced by in vivo electroporation. Proc Natl Acad Sci U S A. 2007; 104:1027–1032. [PubMed: 17209010]

Meredith MM, Liu K, Darrasse-Jeze G, Kamphorst AO, Schreiber HA, Guermonprez P, Idoyaga J, Cheong C, Yao KH, Niec RE, Nussenzweig MC. Expression of the zinc finger transcription factor zDC (Zbtb46, Btbd4) defines the classical dendritic cell lineage. J Exp Med. 2012; 209:1153–1165. [PubMed: 22615130]

Metzger TC, Anderson MS. Control of central and peripheral tolerance by Aire. Immunol Rev. 2011; 241:89–103. [PubMed: 21488892]

Nagamine K, Peterson P, Scott HS, Kudoh J, Minoshima S, Heino M, Krohn KJ, Lalioti MD, Mullis PE, Antonarakis SE, Kawasaki K, Asakawa S, Ito F, Shimizu N. Positional cloning of the APECED gene. Nat Genet. 1997; 17:393–398. [PubMed: 9398839]

Nishikawa Y, Hirota F, Yano M, Kitajima H, Miyazaki J, Kawamoto H, Mouri Y, Matsumoto M. Biphasic Aire expression in early embryos and in medullary thymic epithelial cells before end-stage terminal differentiation. J Exp Med. 2010; 207:963–971. [PubMed: 20404099]

Ross EA, Coughlan RE, Flores-Langarica A, Lax S, Nicholson J, Desanti GE, Marshall JL, Bobat S, Hitchcock J, White A, Jenkinson WE, Khan M, Henderson IR, Lavery GG, Buckley CD, Anderson G, Cunningham AF. Thymic function is maintained during Salmonella-induced atrophy and recovery. J Immunol. 2012; 189:4266–4274. [PubMed: 22993205]

Rossi SW, Kim MY, Leibbrandt A, Parnell SM, Jenkinson WE, Glanville SH, Mcconnell FM, Scott HS, Penninger JM, Jenkinson EJ, Lane PJ, Anderson G. RANK signals from CD4(+)3(−) inducer cells regulate development of Aire-expressing epithelial cells in the thymic medulla. J Exp Med. 2007; 204:1267–1272. [PubMed: 17502664]

Shum AK, Devoss J, Tan CL, Hou Y, Johannes K, O'gorman CS, Jones KD, Sochett EB, Fong L, Anderson MS. Identification of an autoantigen demonstrates a link between interstitial lung disease and a defect in central tolerance. Sci Transl Med. 2009; 1 9ra20.

Stritesky GL, Jameson SC, Hogquist KA. Selection of self-reactive T cells in the thymus. Annu Rev Immunol. 2012; 30:95–114. [PubMed: 22149933]

Su MA, Davini D, Cheng P, Giang K, Fan U, Devoss JJ, Johannes KP, Taylor L, Shum AK, Valenzise M, Meloni A, Bour-Jordan H, Anderson MS. Defective autoimmune regulator-dependent central tolerance to myelin protein zero is linked to autoimmune peripheral neuropathy. J Immunol. 2012; 188:4906–4912. [PubMed: 22490868]

Su MA, Giang K, Zumer K, Jiang H, Oven I, Rinn JL, Devoss JJ, Johannes KP, Lu W, Gardner J, Chang A, Bubulya P, Chang HY, Peterlin BM, Anderson MS. Mechanisms of an autoimmunity syndrome in mice caused by a dominant mutation in Aire. J Clin Invest. 2008; 118:1712–1726. [PubMed: 18414681]

Taniguchi RT, Devoss JJ, Moon JJ, Sidney J, Sette A, Jenkins MK, Anderson MS. Detection of an autoreactive T-cell population within the polyclonal repertoire that undergoes distinct autoimmune regulator (Aire)-mediated selection. Proc Natl Acad Sci U S A. 2012; 109:7847–7852. [PubMed: 22552229]

Villasenor J, Besse W, Benoist C, Mathis D. Ectopic expression of peripheral-tissue antigens in the thymic epithelium: probabilistic, monoallelic, misinitiated. Proc Natl Acad Sci U S A. 2008; 105:15854–15859. [PubMed: 18836079]

Wang X, Laan M, Bichele R, Kisand K, Scott HS, Peterson P. Post-Aire maturation of thymic medullary epithelial cells involves selective expression of keratinocyte-specific autoantigens. Front Immunol. 2012; 3:19. [PubMed: 22448160]

White AJ, Nakamura K, Jenkinson WE, Saini M, Sinclair C, Seddon B, Narendran P, Pfeffer K, Nitta T, Takahama Y, Caamano JH, Lane PJ, Jenkinson EJ, Anderson G. Lymphotoxin signals from positively selected thymocytes regulate the terminal differentiation of medullary thymic epithelial cells. J Immunol. 2010; 185:4769–4776. [PubMed: 20861360]

White AJ, Withers DR, Parnell SM, Scott HS, Finke D, Lane PJ, Jenkinson EJ, Anderson G. Sequential phases in the development of Aire-expressing medullary thymic epithelial cells involve distinct cellular input. Eur J Immunol. 2008; 38:942–947. [PubMed: 18350550]

Yano M, Kuroda N, Han H, Meguro-Horike M, Nishikawa Y, Kiyonari H, Maemura K, Yanagawa Y, Obata K, Takahashi S, Ikawa T, Satoh R, Kawamoto H, Mouri Y, Matsumoto M. Aire controls the differentiation program of thymic epithelial cells in the medulla for the establishment of self-tolerance. J Exp Med. 2008; 205:2827–2838. [PubMed: 19015306]

Zuklys S, Balciunaite G, Agarwal A, Fasler-Kan E, Palmer E, Hollander GA. Normal thymic architecture and negative selection are associated with Aire expression, the gene defective in the autoimmunepolyendocrinopathy- candidiasis-ectodermal dystrophy (APECED). J Immunol. 2000; 165:1976–1983. [PubMed: 10925280]

Highlights

- Aire-DTR mice allow efficient ablation of Aire+ mTECs
- Repeated ablation in Aire-DTR mice leads to loss of mTEC subsets
- Fate mapping reveals a large population of post-Aire mTECs
- Post-Aire mTECs retain intermediate TSA expression and lose maturation markers

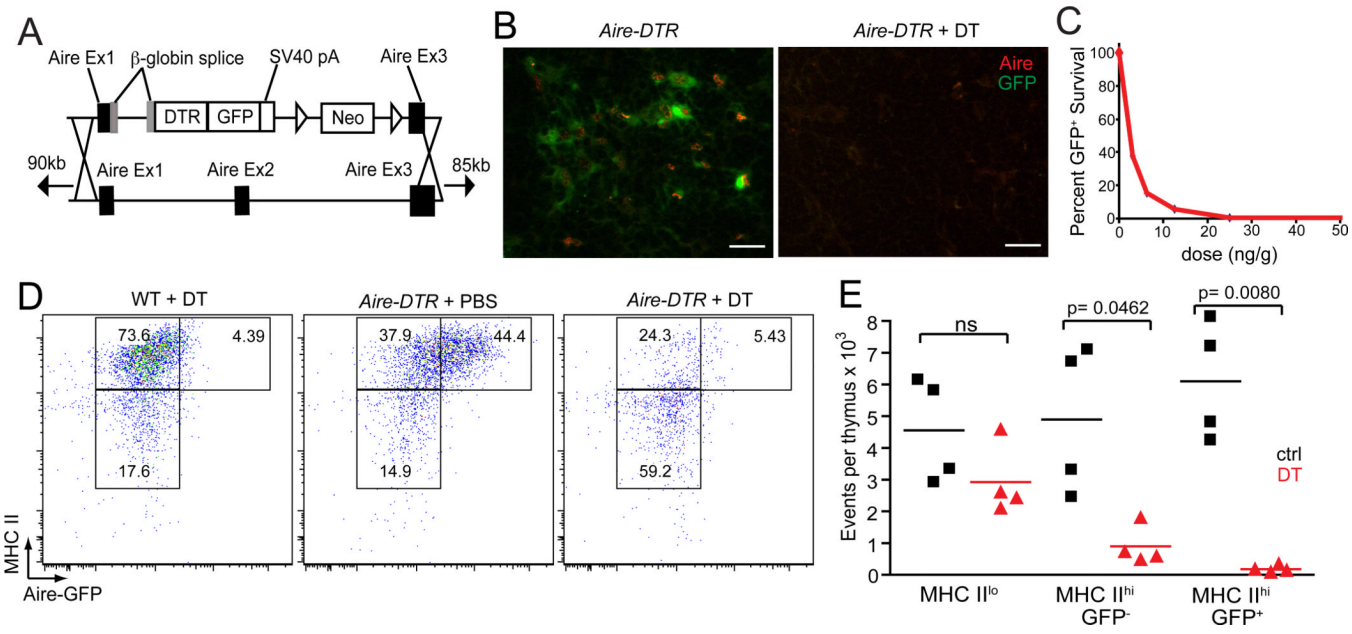

Figure 1.

The *Aire-DTR* mouse facilitates efficient ablation of Aire$^+$ mTECs. (**A**) Schematic of the *Aire-DTR* transgene targeting expression of a DTR-GFP fusion protein to a 175 kb BAC containing the murine Aire locus. (**B**) Immunofluorescent staining of GFP (green) and Aire (red) in thymic sections from *Aire-DTR* mice, 24 hours after a single dose of 50 ng/g DT (+DT). Scale bars = 25 μm. Representative of two independent experiments. (**C**) Percent GFP$^+$ MHCII$^+$ CD45$^-$ mTEC survival after two daily injections of the indicated DT dose, standardized to untreated *Aire-DTR* controls. (**D**) Flow cytometric analysis of MHC II and GFP expression in mTECs (CD45$^-$, EpCAM$^+$, Ly51$^-$) from the indicated mice 24 hours after one dose of 50 ng/g DT. Representative of two independent experiments, n=4. (**E**) Quantification of (**D**), showing total events per thymus of the indicated mTEC subsets.

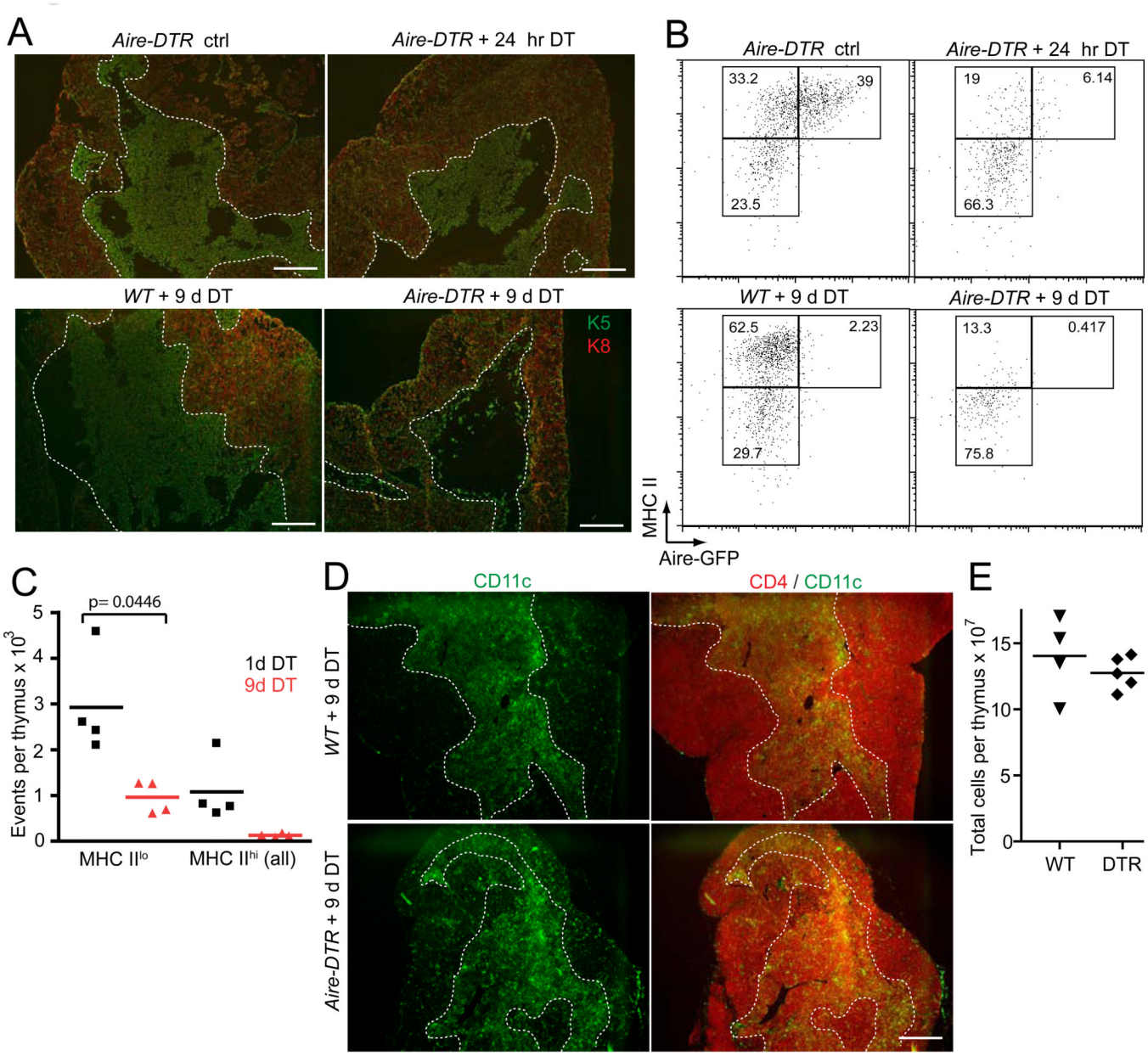

Figure 2.

Extended Aire$^+$ mTEC ablation depletes all mTEC subsets. (**A**) Immunofluorescent staining of thymi from mice receiving 50 ng/g DT either once (24 hours) or five times (over 9 days) stained for cytokeratins 5 and 8 (K5, green; K8, red). Broken lines indicate the cortico-medullary junction. Scale bars = 400 μm. Representative of three independent experiments. (**B**) Flow cytometric analysis of MHC class II and GFP expression in mTECs (CD45$^-$, EpCAM$^+$, Ly51$^-$) from same conditions in (**A**). (**C**) Quantification of (**B**), showing total events per thymi of the *Aire-DTR* mice, from two independent cohorts of mice, n=4. (**D**) Immunofluorescence images of CD11c (green) and CD4 (red) staining of thymic sections from wild-type and *Aire-DTR* mice given repeated DT injections. Broken lines indicate the cortico-medullary junction. Scale bars = 400 μm. Representative of three independent experiments. (**E**) Total thymic cellularity from littermate wild-type and *Aire-DTR* mice after receiving repeated DT treatment, from two independent cohorts.

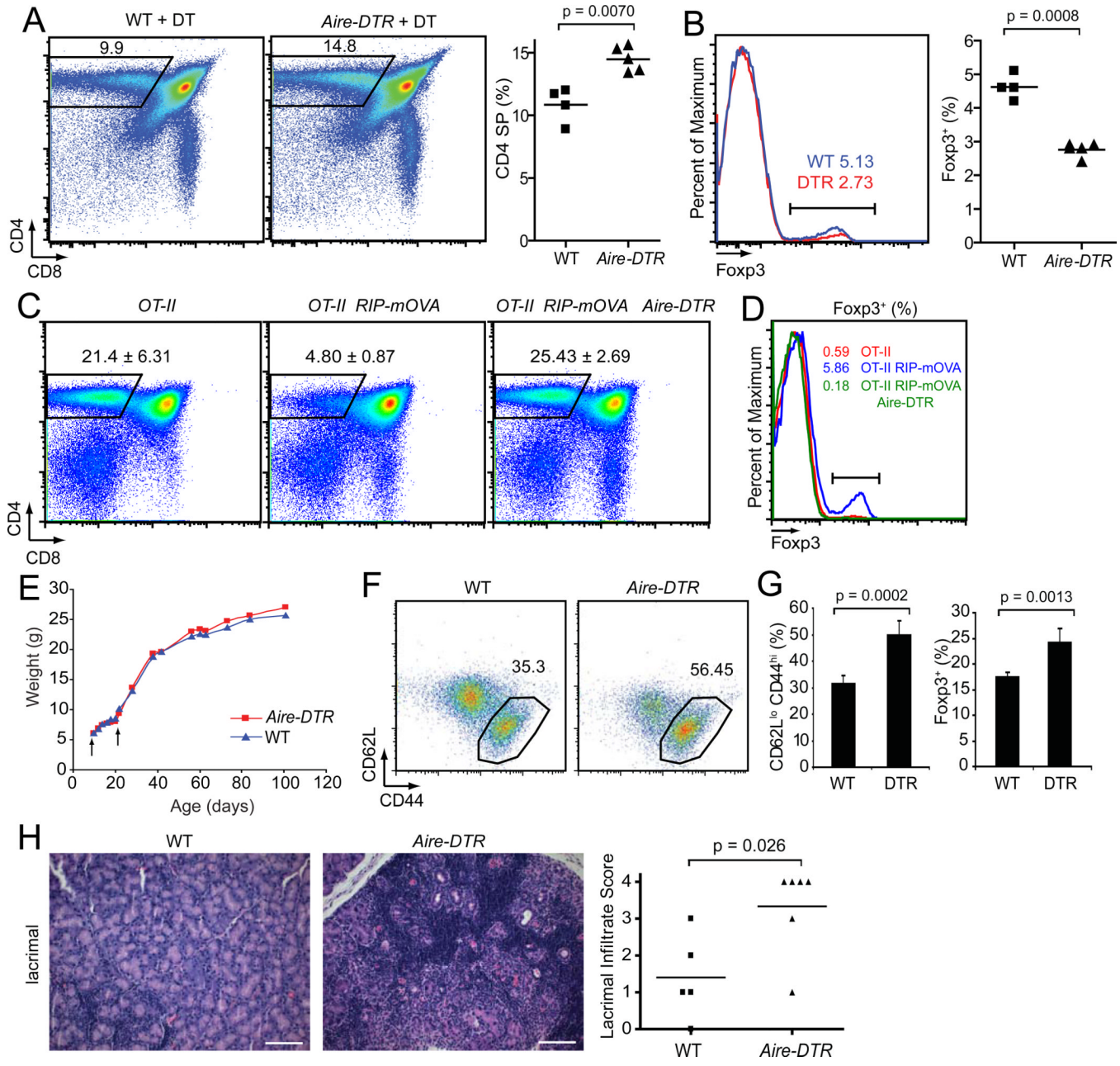

Figure 3.

mTEC ablation leads to impaired CD4$^+$ T cell selection and autoimmunity. (**A**) Flow cytometric plots of CD4 and CD8 staining and percents of CD4 SP events of thymocytes in female mice of the indicated genotype at the end of repeated DT treatment. Data are representative of three independent experiments. (**B**) Histograms of Foxp3 staining among CD4 SP fractions shown in (**A**) for either wild-type (blue) or *Aire-DTR* (red) mice. (**C**) Flow cytometric plots of CD4 and CD8 staining and percents of CD4 SP events of thymocytes in mice of the indicated genotype at the end of repeated DT treatment. Mean +/− SD CD4 SP percent is shown for 3-4 mice per group from two independent experiments. (**D**) Representative histograms of Foxp3 staining among CD4 SP events gated in (**C**). (**E**) Plot of mean weights over time of a cohort of 5-6 mice of each indicated genotype. 25 ng/g DT was given i.p. every 48 hours between 7 and 21 days. (**F**) Representative flow cytometric plot of

CD44 and CD62L staining of $CD4^+$ splenocytes analyzed at 14 weeks of age. (**G**) Quantification of (**F**) for the cohort of mice in (**E**), left, and quantification of Foxp3+ (%) events among $CD4^+$ splenocytes for the same cohort of mice. Mean + SD. (**H**) Representative histological analyses of lacrimal glands from mice in (**E**) stained with hematoxylin and eosin (left) and infiltrate scores for the same cohort of mice (right). Scale bars = 100 μm. See also Figure S1.

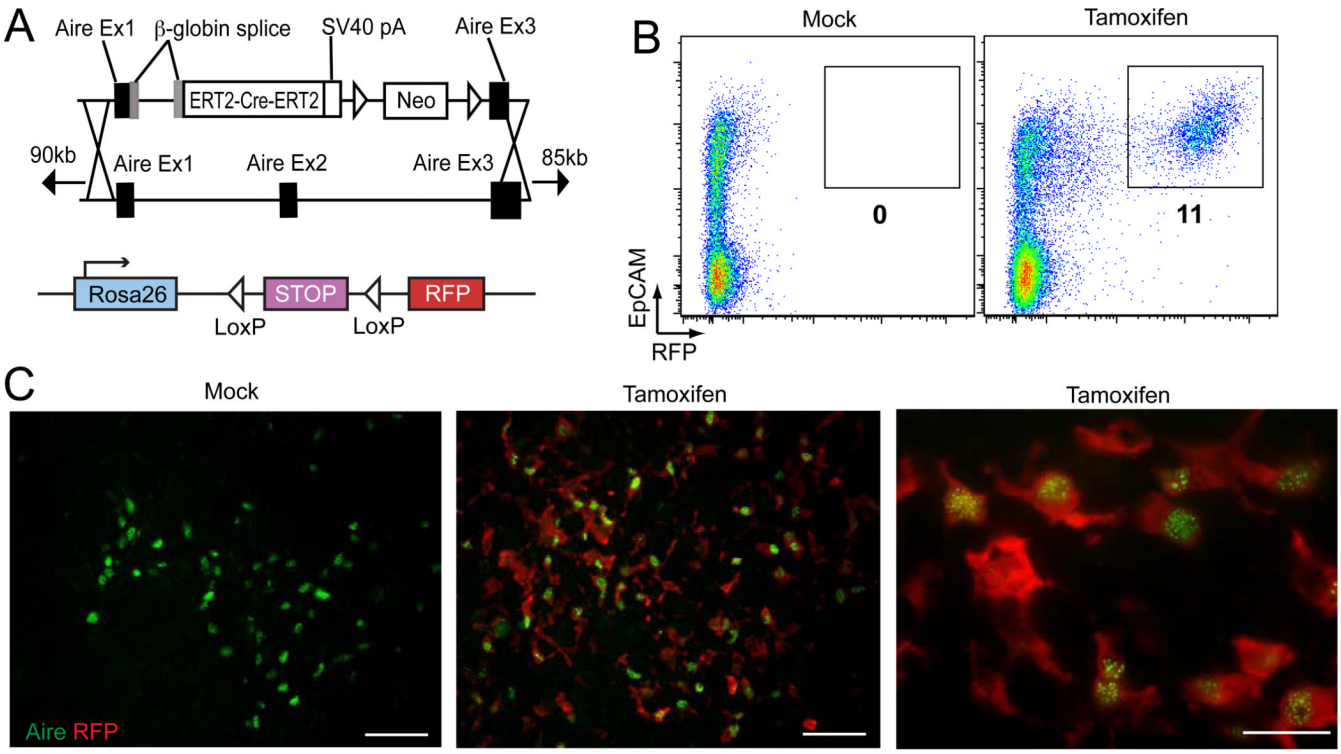

Figure 4.

The *Aire-Cre* mouse allows inducible labeling of *Aire*-expressing mTECs. (**A**) Schematic of the *Aire-Cre* transgene targeting expression of an ERT2-Cre-ERT2 fusion protein to Aire^{+} cells through a 175 kb BAC containing the Aire locus (top). When crossed with the Ai14 Rosa26 RFP mice (bottom), tamoxifen-induced Cre activity excises the stop codon to allow constitutive RFP (TdTomato) expression. (**B**) Flow cytometric analysis of thymic stromal fractions from *Aire-Cre x Ai14* mice given 7 mg tamoxifen or corn oil at day 0 and day 3 and analyzed on day 5. Plots show EpCAM and RFP signal on CD45^{-} events. (**C**) Representative immunofluorescent staining of Aire and RFP from thymic sections of the same mice as (**B**), with mock corn oil or tamoxifen injections indicated. Scale bars = 50 μm, left and middle, 20 μm, right.

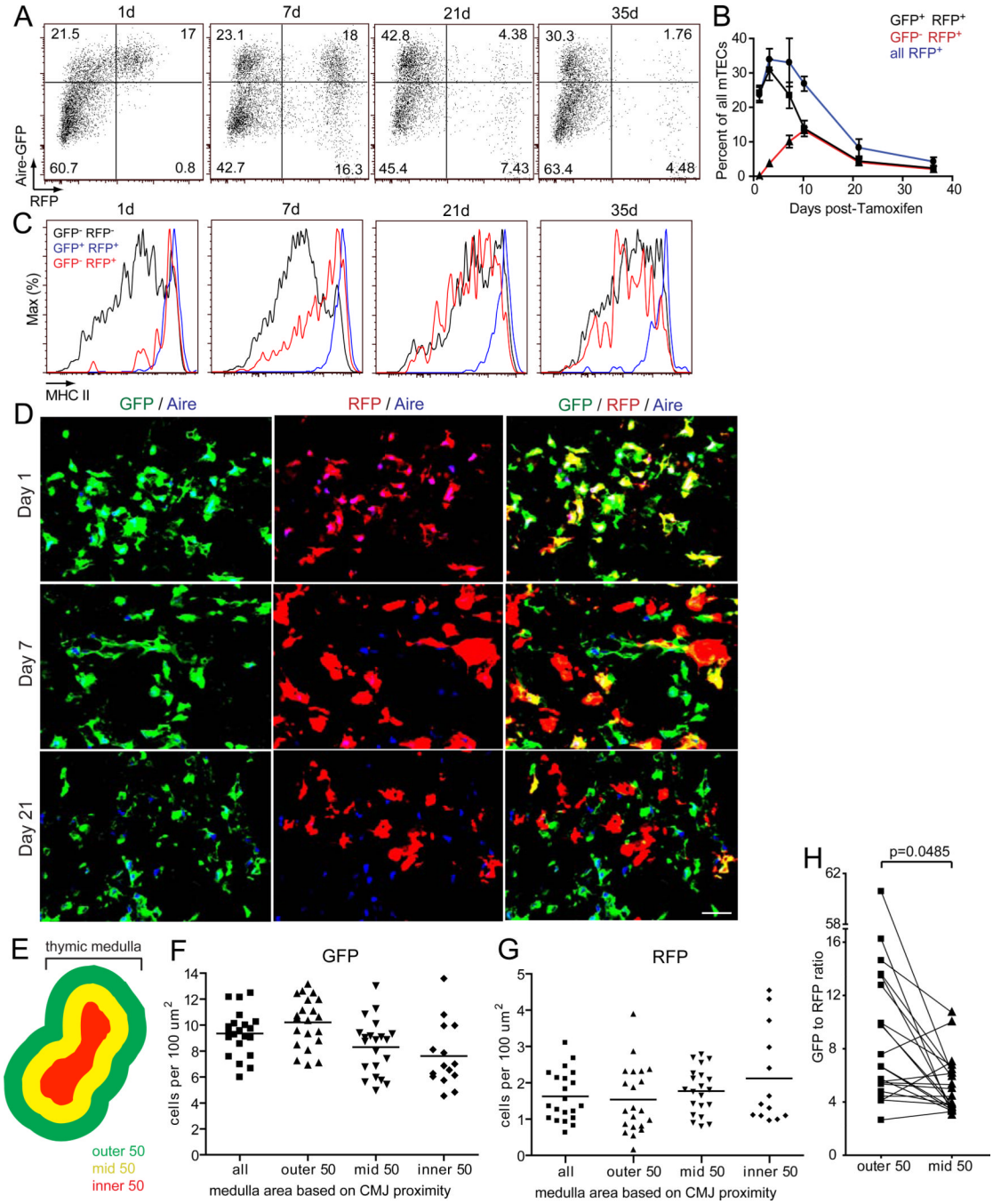

Figure 5.

Post-Aire mTECs downregulate MHC Class II. (**A**) Flow cytometric analyses of *Aire-Cre x Ai14(*Rosa26-RFP) *x Aire-GFP* (*Adig Aire*-reporter) mice treated with 2 mg tamoxifen at d0 and analyzed at the indicated timepoints. Plots are pre-gated on $CD11c^{-}$, $CD45^{-}$, $EpCAM^{+}$ events, and representative of two independent experiments, n=4. (**B**) Plots from mice analyzed as in (**A**), showing mean +/- SD over time of indicated populations, pooled from four independent experiments. (**C**) Representative histograms of MHC II expression by indication GFP vs. RFP subsets gated in (**A**). (**D**) Representative immunofluorescent analyses of thymi from mice shown in (**A**) with overlays of GFP (green), RFP (red) and/or

Aire (blue) as indicated. Scale bar = 50 μm. (**E**) Schematic of sub-regions of the medulla for which densities were calculated in the following displays. Concentric 50 um regions starting from the cortico-medullary boundary were defined, with the outer region most proximal to the boundary, and the density of mTEC subsets within each region was determined. (**F**) Calculation of GFP^+ mTEC densities (cells per 100 um^2) among the entire medullary region (all) and within the three concentric regions depicted in (**E**). Data are from 21 medullary regions imaged from four separate thymi of *Aire-Cre x Ai14(*Rosa26-RFP) *x Aire-GFP* (*Adig Aire*-reporter) mice 21 days after tamoxifen treatment. (**G**) Calculation of RFP+ mTEC densities as in (**F**). (**H**) Comparison of the ratio of GFP and RFP densities across the outer and mid regions showed statistical significance using a paired t-test. See also Figure S2.

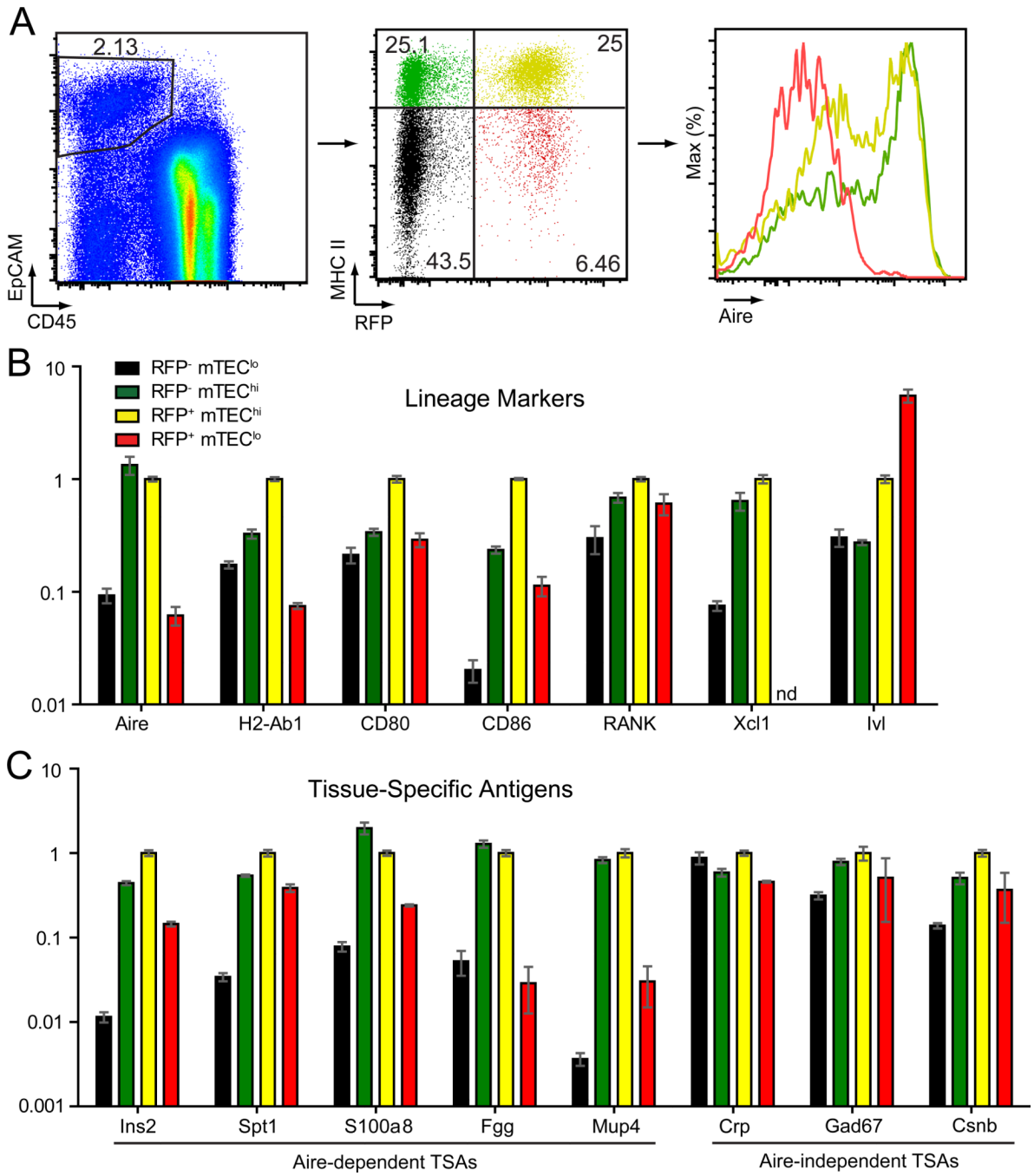

Figure 6.

Post-Aire mTECs lose maturation markers but maintain intermediate TSA expression. (**A**) Representative flow cytometric analysis of an *Adig x Aire-Cre x Ai14* (Rosa26-RFP) mouse treated with tamoxifen 7 days prior to analysis. mTECs were identified as CD11c- (not shown) and CD45^{-} EpCAM^{+} (left). A polychromatic plot shows the distribution of MHCII (green) and RFP (red) signal among TECs (middle), and Aire staining of the indicated quadrants (MHCII^{hi} RFP^{-}, green; MHCII^{hi} RFP^{+}, yellow; MHCII^{lo}, RFP^{+}, red) is shown to the right, demonstrating the lack of Aire expression among RFP^{+} MHCII^{lo} events. (**B**) Quantitative PCR analyses of indicated maturation targets (H2-Ab1 = MHC Class II; Ivl =

Involucrin; RANK = Tnfrsf11a; OPG = Tnfrsf11b) on populations depicted in (**A**). Results are representative of 2 or 3 independent sorts. Mean +/- SD. (**C**) Quantitative PCR analyses of indicated Aire-dependent TSA targets (left) and Aire-independent TSAs on populations depicted in (**A**). Crp = C-reactive protein; Gad67 = Gad1; Csnb = Csn2, casein beta. Results are representative of 2 or 3 independent sorts. Mean +/− SD.

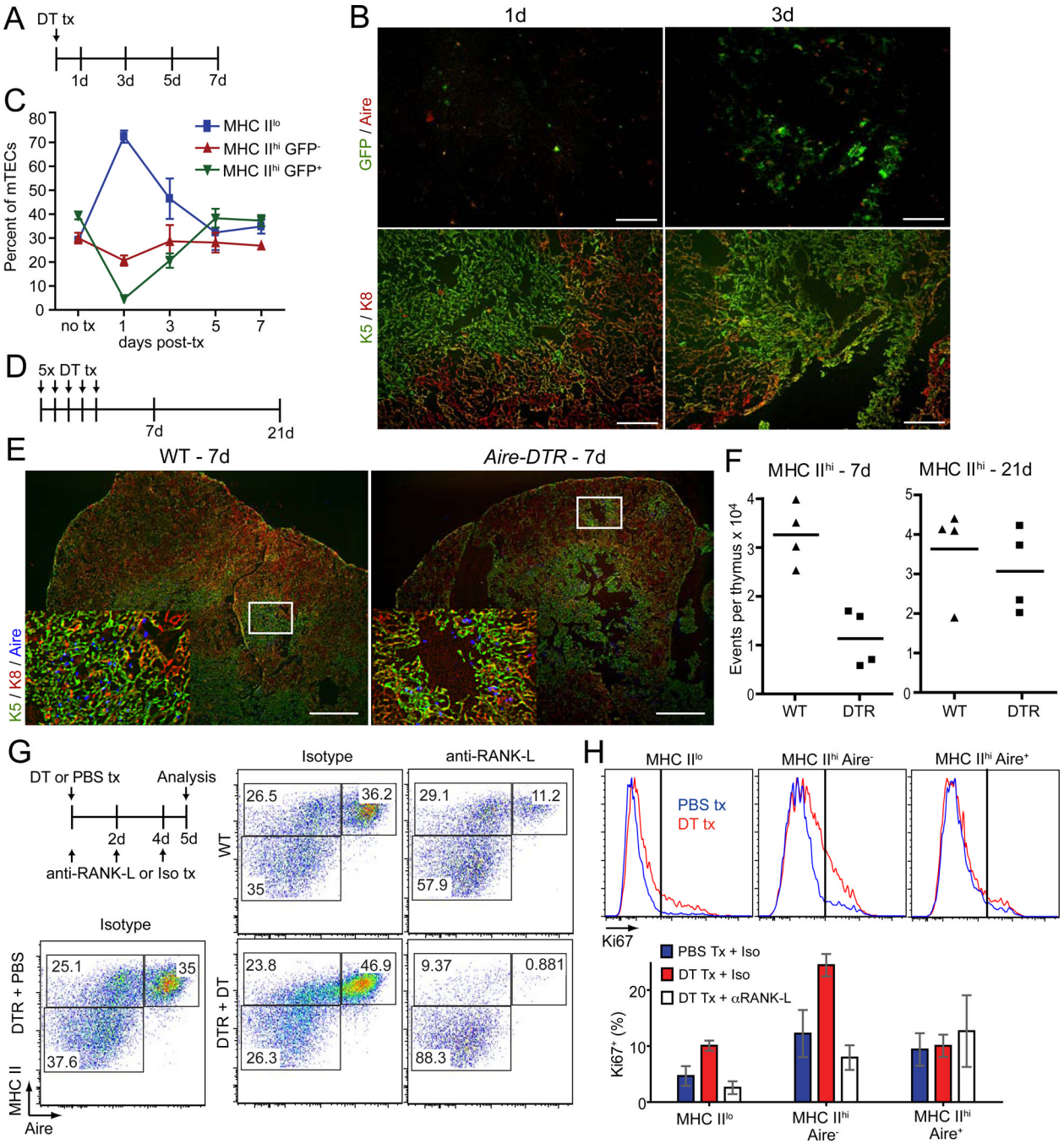

Figure 7.

RANK signaling controls Aire$^+$ mTEC development. (**A**) Schematic of single DT treatment (50 ng/g) of *Aire-DTR* mice and subsequent timepoints of analysis. (**B**) Immunofluorescent analysis of serial sections from mice after 1 or 3 days of recovery, with GFP (green) and Aire (red) above, or cytokeratin 5 (K5; green) and cytokeratin 8 (K8; red). Scale bars = 100 μm. Representative of three independent experiments. (**C**) Quantification of flow cytometric analysis of thymi at the indicated timepoints of recovery from DT treatment, showing mean +/− SD of the percent of mTECs in either MHC II lo, MHC II lo GFP−, or MHC II lo GFP+ gates. n=4 per timepoint, pooled from two independent experiments. (**D**) Schematic of

repeated DT treatment and recovery analysis at one or three weeks after the end of DT treatment. (**E**) Representative immunofluorescent staining of K5 (green), K8 (red), or Aire (blue) in thymic sections of the indicated genotype after one week of recovery from mTEC ablation. Scale bars = 400 um. (**F**) Quantification of flow cytometric analysis of thymi at the indicated timepoints of recovery from mTEC ablation, showing mean and SD of the total numbers of MHC II^{hi} mTECs per thymus. (**G**) Schematic of DT treatment and i.p. injections of either anti-RANK-L or isotype control (upper left) followed by analysis after 5 days of recovery (upper left), and representative flow cytometric of MHC II and Aire staining of $CD11c^{-}$, $CD45^{-}$, $EpCAM^{+}$ mTECs from indicated mice. n=4 per condition. (**H**) Representative histograms of Ki67 staining of populations in (**G**) for PBS (blue) or DT (red) treated, isotype treated DTR^{+} mice (top), and quantification of mean +/− SD of percent Ki67+ events among the indicated mTEC subsets from DTR^{+} mice receiving indicated treatments.